Theoretical and Computational Fluid Dynamics manuscript No.
(will be inserted by the editor)

Jonathan Gustafsson · Bartosz Protas

On Oseen Flows for Large Reynolds Numbers

Received: date / Accepted: date

Abstract This investigation offers a detailed analysis of solutions to the two–dimensional Oseen problem in the exterior of an obstacle for large Reynolds numbers. It is motivated by mathematical results highlighting the important role played by the Oseen flows in characterizing the asymptotic structure of steady solutions to the Navier–Stokes problem at large distances from the obstacle. We compute solutions of the Oseen problem based on the series representation discovered by Tomotika and Aoi [8] where the expansion coefficients are determined numerically. Since the resulting algebraic problem suffers from very poor conditioning, the solution process involves the use of very high arithmetic precision. The effect of different numerical parameters on the accuracy of the computed solutions is studied in detail. While the corresponding inviscid problem admits many different solutions, we show that the inviscid flow proposed by Stewartson [38] is the limit that the viscous Oseen flows converge to as $Re \to \infty$. We also draw some comparisons with the steady Navier–Stokes flows for large Reynolds numbers.

Keywords Oseen equation · External Flows · Wakes · Steady Flows · Computational Methods

PACS 47.15.Tr · 47.54.Bd

1 Introduction

This research concerns steady incompressible flows past obstacles in unbounded domains and we investigate solutions of Oseen's approximation to the Navier–Stokes system in the limit of vanishing viscosities. Motivated by certain mathematical results highlighting the role of the Oseen problem for some open questions in theoretical hydrodynamics, we will attempt to provide a modern look at this classical problem. We consider two–dimensional (2D) flows past a circular cylinder A with the unit radius in an unbounded domain $\Omega \triangleq \mathbb{R}^2 \backslash \overline{A}$ ("$\triangleq$" means "equal to by definition"). It is assumed that

Jonathan Gustafsson
School of Computational Engineering & Science, McMaster University, Hamilton, Ontario, Canada
Tel.: +1 905-525-9140, ext. 24411
Fax: +1 905-522-0935
E-mail: Jonathan.Gustafsson@math.mcmaster.ca

Bartosz Protas
Department of Mathematics & Statistics, McMaster University, Hamilton, Ontario, Canada
Tel.: +1 905-525-9140, ext. 24116
Fax: +1 905-522-0935
E-mail: bprotas@mcmaster.ca

the flow is generated by the free stream $\mathbf{u}_\infty = 1\,\mathbf{e}_x$ at infinity, where $\mathbf{e}_x$ is the unit vector associated with the OX axis. Denoting $\mathbf{u} = [u, v]^T$ the velocity field, p the pressure, and assuming the fluid density is equal to unity, the Oseen system takes the following form

$$\mathbf{u}_\infty \cdot \boldsymbol{\nabla}\mathbf{u} + \boldsymbol{\nabla} p - \frac{1}{Re}\Delta\mathbf{u} = \mathbf{0} \qquad \text{in } \Omega, \tag{1a}$$

$$\boldsymbol{\nabla} \cdot \mathbf{u} = 0 \qquad \text{in } \Omega, \tag{1b}$$

$$\mathbf{u} = \mathbf{0} \qquad \text{on } \partial A, \tag{1c}$$

$$\mathbf{u} \to \mathbf{u}_\infty \quad \text{as } |\mathbf{x}| \to \infty, \tag{1d}$$

where $\mathbf{x} = [x, y]^T$ is the position vector, Re denotes the Reynolds number. The coordinate system is fixed at the obstacle and the no–slip boundary conditions were assumed at the obstacle boundary ∂A. Noting that the obstacle diameter is $d = 2$, the Reynolds number is calculated as

$$Re = \frac{2|\mathbf{u}_\infty|}{\mu}, \tag{2}$$

where μ is the dynamic viscosity. System (1) is a linearization of the Navier–Stokes problem obtained by replacing the advection velocity in the nonlinear term with the free stream $\mathbf{u}_\infty$. It therefore represents an alternative model to the Stokes approximation in which the nonlinear term is eliminated entirely, resulting in a problem which admits no solutions in 2D, a fact known as Stokes' paradox [1]. While the time–dependent generalizations were recently considered [2], Oseen's linearization, as well as Stokes', is typically studied in the time–independent setting.

In the '50s and '60s the Oseen equation generated significant interest, since being analytically tractable, its solutions offered valuable quantitative insights into properties (such as, e.g., drag) of low–Reynolds number flows past bluff bodies, otherwise unavailable in the pre–CFD era. Different solutions of the Oseen equation, either in 2D or in 3D, were constructed by Lamb [3], Oseen himself [4], Burgess [5], Faxén [6] and Goldstein [7] to mention the first attempts only. It should be, however, emphasized that these early "solutions" satisfied governing equation (1a), or boundary condition (1c), or both, in an approximate sense only. The first solution (in the 2D case for the flow past a circular cylinder) satisfying exactly both the governing equation and the boundary conditions, albeit depending on an infinite number of constants, is that of Faxén [6]. It was later rederived in simpler terms by Tomotika and Aoi [8], whereas Dennis and Kocabiyik [9] obtained analogous solutions for flows past elliptic cylinders inclined with respect to the oncoming flow. We also mention the work of Chadwick et al. [10,11] who considered solutions expressed in terms of convolution integrals with "Oseenlets", i.e., Green's functions for equation (1). Even a cursory survey of these results and the different applications that the Oseen equation found in the studies of wake flows, both fundamental and applied, is beyond the scope of this paper. Instead, we refer the reader to the excellent historical reviews by Lindgren [12] and Veysey II & Goldenfeld [13], and the monograph by Berger [14] for a survey of historical developments and different applications. Following the advent of computational fluid dynamics which made it possible to solve the complete Navier–Stokes system numerically, the interest in the Oseen approximation as a means of studying real flows subsided. We remark that the Oseen system is still occasionally used as a testbed for validating different computational approaches (e.g., stabilization of finite element discretizations [15], or artificial boundary conditions on truncated computational domains [16]).

The present investigation reflects a renewed interest in the Oseen system which comes from a somewhat different direction. It is motivated by certain results of the mathematical analysis concerning the far–wake structure in the steady–state solutions of the Navier–Stokes equation in unbounded domains. The related question of the asymptotic, as $Re \to \infty$, structure of the separated 2D flow past a bluff body was studied extensively using methods of the asymptotic analysis since the 1960s. A number of different limiting solutions have been proposed which fall into two main categories illustrated schematically in Figure 1, namely, flows characterized by slender wakes extending to infinity such as the Kirchhoff–type

solutions with free streamlines [17,18], and flows with wide closed wakes reminiscent of the Prandtl–Batchelor limiting solution [19] with two counter–rotating vortices attached to the obstacle. However, the only asymptotic solution which has been found to be self–consistent and which has withstood the test of time is that of Chernyshenko [20], see also [21]. It features two large recirculation regions with the width and length growing proportionally to Re and the drag coefficient decreasing to zero with Re. This type of asymptotic solution was later generalized in different directions, namely, for flows past rows of obstacles in [22] and for flows with stratification in [23]. As concerns computational studies, the work of Fornberg [24,25] was pioneering and still represents the state–of–the–art in this area. More recently it was followed by computational studies of steady flows past rows of obstacles in [26,27] and flows past obstacles in channels [28], whereas steady three–dimensional (3D) flows past a sphere were studied in [29]. The results of Fornberg [25] for Reynolds numbers up to about 300 feature a slender elongated wake bubble, whereas for higher values of the Reynolds number, these solutions develop a significantly wider wake consistent with the theory of Chernyshenko [20,21]. Flows with similar structure were also found in [26,27] in the case of a large distance between the obstacles. As regards the behavior of the drag, the computations of Fornberg [25] indicated the vanishing of the drag coefficient with $Re \to \infty$. The history of different research efforts concerning this problem and based on the asymptotic analysis and computations is surveyed in the review papers [21] and [30], respectively, whereas monograph [31] offers a broad overview of asymptotic methods applied to the study of separated flows. An ultimate goal of our research is to recompute steady 2D flows past an obstacle for Reynolds numbers significantly higher than investigated by Fornberg quarter of a century ago and using computational techniques which leverage certain rigorous analytical results available for this problem which we review briefly below. There are also some intriguing questions concerning possible nonuniqueness of solutions to this problem.

Let $\mathbf{U}$ denote the solution of the steady Navier–Stokes problem, to be distinguished from $\mathbf{u}$ satisfying Oseen system (1). A key mathematical result established by Finn [32] and Smith [33], and discussed at length in the monograph by Galdi [34], states that solutions of the steady–state Navier–Stokes equations whose properties conform to what is actually observed in real flows (e.g., nonzero drag) and hence referred to as "physically reasonable" (PR), have in 2D the following asymptotic behavior for $|\mathbf{x}| \to \infty$ [34, Theorem 6.1 in Volume II]

$$\mathbf{U}(\mathbf{x}) = \mathbf{u}_\infty + \mathbf{E}(\mathbf{x}) \cdot \mathbf{F} + \mathbf{W}(\mathbf{x}), \tag{3}$$

where $\mathbf{E}(\mathbf{x})$ is the Oseen fundamental tensor, $\mathbf{F}$ is the hydrodynamic force acting on the obstacle A, whereas the field $\mathbf{W}(\mathbf{x})$ satisfies the estimate $|\mathbf{W}(\mathbf{x})| \sim \mathcal{O}(|\mathbf{x}|^{-1+\epsilon_1})$ for some arbitrarily small $\epsilon_1 > 0$. The Oseen tensor $\mathbf{E}(\mathbf{x})$ is a fundamental solution of Oseen equation (1a)–(1b). Its construction and properties, especially in regard to the slow asymptotic decay at infinity, are reviewed in detail in [34, Volume I]. Relation (3) thus implies that the difference $|\mathbf{U} - \mathbf{u}_\infty|$ vanishes relatively slowly with $|\mathbf{x}|$, i.e., as $\mathcal{O}(|\mathbf{x}|^{-\frac{1}{2}})$ along the flow center line. It should be emphasized that this behavior is markedly different from the corresponding behavior of solutions in time–dependent 2D Navier–Stokes system in unbounded domains where the difference $(\mathbf{U} - \mathbf{u}_\infty)$ decays in fact significantly faster [35]. Analogous differences between the asymptotic properties of the steady and time–dependent solutions also exist in 3D. We wish to stress that the properties mentioned above, in particular (3), are not hypotheses or assumptions, but rigorously established mathematical facts concerning the Navier–Stokes system. Relation (3) is in fact quite important as it represents a property, admittedly rather difficult to verify in numerical computations, which characterizes all PR solutions. We emphasize that this is a rather nontrivial issue and it is not obvious whether the computational solutions discussed above actually possess the PR property. Ideas related to incorporating Oseen asymptotics (3) into the far–field boundary conditions in the numerical solution of the steady–state Navier–Stokes system were pursued by Fornberg [24,25] and also more recently in [36,37], although this concept can be traced back at least to [32]. Our objective in this paper is to explore the properties of the solutions to Oseen system (1) for a broad range of

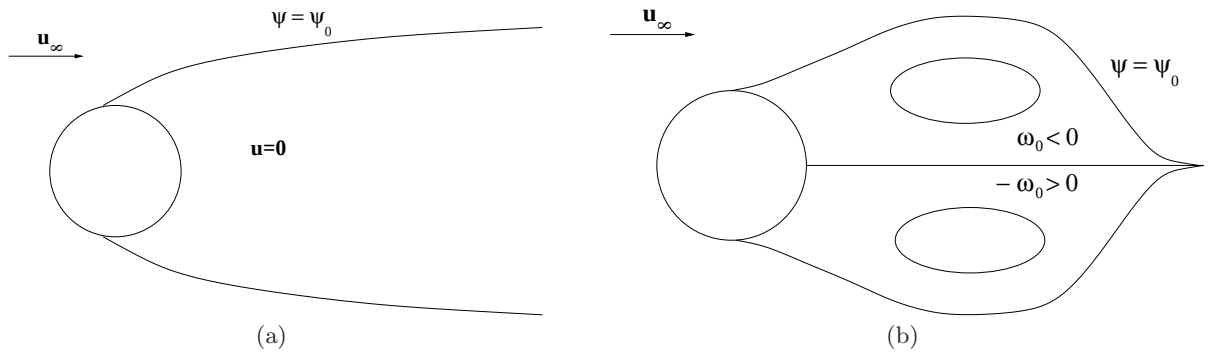

Fig. 1 Schematic showing the main features of the separation zone in (a) Kirchhoff's model and (b) Batchelor's model of the steady wake flow in the infinite Reynolds number limit.

Reynolds numbers. We will also show that the solution of the inviscid problem proposed by Stewartson [38] is in fact the suitable limit of solutions of the Oseen system as $Re \to \infty$, a result interesting in its own right.

The solution of Oseen equation (1a) found by Tomotika and Aoi [8] has the following form in the polar coordinate system (r, θ) in which $\mathbf{u} = u_r\,\mathbf{e}_r + u_\theta\,\mathbf{e}_\theta$ ($\mathbf{e}_r$ and $\mathbf{e}_\theta$ are the unit vectors in the radial and azimuthal direction, respectively)

$$u_r(r,\theta) = \cos(\theta) - \frac{\partial \phi}{\partial r} + \frac{1}{2k}\frac{\partial \chi}{\partial r} - \chi\cos\theta, \tag{4a}$$

$$u_\theta(r,\theta) = -\sin(\theta) - \frac{1}{r}\frac{\partial \phi}{\partial \theta} + \frac{1}{2kr}\frac{\partial \chi}{\partial \theta} + \chi\sin\theta, \tag{4b}$$

where

$$\chi(r,\theta) = e^{kr\cos\theta}\sum_{m=0}^{\infty} B_m K_m(kr)\cos m\theta, \tag{5a}$$

$$\phi(r,\theta) = A_0\log r - \sum_{n=1}^{\infty}\frac{A_n}{n}\frac{\cos n\theta}{r^n}, \tag{5b}$$

in which $k \triangleq \frac{Re}{4}$, K_m are the modified Bessel functions of the second kind and of order m, and A_n, B_m, $m, n = 0, 1, \ldots$ are a priori undetermined constants. By "obtaining a solution" we mean finding suitable truncations of the series in (5a) and (5b), and determining the corresponding finite sets of constants A_n, $n = 0, \ldots, N$ and B_m, $m = 0, \ldots, M$, such that boundary condition (1c) on the surface of the cylinder is satisfied to an acceptable accuracy. As will be demonstrated below, this seemingly straightforward task leads in fact to a number of computational difficulties. Since, other than a very early investigation [39], such solutions do not seem to have ever been thoroughly studied, our goal in this research is to employ modern methods of scientific computing to investigate these solutions in detail for a broad range of the Reynolds number. More specifically, we would like to address the following problems:

1. determination of the coefficients A_n and B_m in a computationally efficient manner; in view of the very poor conditioning of the underlying algebraic system and the difficulties involved in evaluating high–order modified Bessel function of the second kind, this is a rather nontrivial issue,
2. establishing convergence of series appearing in (5a) and (5b); solutions (4) are only "formal", in the sense that it is not a priori evident whether the series defining χ and ϕ converge; in the absence of relevant analytical results, we will address this issue computationally,
3. properties of solutions (4), especially in regard to the structure of the wake, for large values of the Reynolds number and the existence of a suitable inviscid limit.

We add that the early approximate solutions of Oseen problem (1) given in [3–5] essentially correspond to one–term truncations of series in (5a)–(5b), whereas the solutions reported in [9] utilized four terms. The structure of the paper is as follows: in the next Section we discuss the algebraic system that needs to be solved to obtain solution (4), in Section 3 we recall and discuss the flow proposed as the inviscid limit of solutions of system (1), whereas in Section 4 we present a range of computational results, conclusions are deferred to Section 5. Some more technical material pertaining to convergence of series in (5) is collected in Appendix A.

2 Series Solution of Oseen Problem

We begin by examining the behavior of series solutions (4a) and (4b) at large distances r from the obstacle. Using the asymptotic expansions of the modified Bessel functions K_m for $r \to \infty$ in (5a), cf. [45], we obtain for the radial and azimuthal velocity components

$$|u_r - \cos\theta| \sim \begin{cases} \frac{1}{\sqrt{r}}, & \text{if } \theta = 0, \\ \frac{1}{r}, & \text{elsewhere.} \end{cases} \tag{6a}$$

$$|u_\theta + \sin\theta| \sim \frac{1}{r^2}, \tag{6b}$$

where "$\sim$" means "proportional to when $r \to \infty$". We note that relations (6) represent indeed the slow asymptotic decay known to characterize the behavior of the solutions of the Oseen equation, cf. [34].

Series solutions (4a) and (4b) depend on two infinite sets of coefficients A_n and B_m, $n, m = 0, 1, \ldots$. Following [8], it is possible to eliminate the coefficients A_n, so that the expressions for the velocity components become

$$u_r = \cos(\theta) - \frac{\cos(\theta)}{r^2} + \frac{1}{4}\sum_{m=0}^{\infty} B_m \sum_{n=1}^{\infty}\left[\frac{\Phi_{m,n}\left(\frac{Re}{4}\right)}{r^{n+1}} - \Phi_{m,n}\left(r\,\frac{Re}{4}\right)\right]\cos(n\theta), \tag{7a}$$

$$u_\theta = -\sin(\theta) - \frac{\sin(\theta)}{r^2} + \frac{1}{4}\sum_{m=0}^{\infty} B_m \sum_{n=1}^{\infty}\left[\frac{\Phi_{m,n}\left(\frac{Re}{4}\right)}{r^{n+1}} - \Psi_{m,n}\left(r\,\frac{Re}{4}\right)\right]\sin(n\theta), \tag{7b}$$

where

$$\begin{aligned}\Phi_{m,n}(kr) &= [K_{m+1}(kr) + K_{m-1}(kr)][I_{m-n}(kr) + I_{m+n}(kr)] \\ &\quad + K_m(kr)[I_{m-n-1}(kr) + I_{m-n+1}(kr) + I_{m+n-1}(kr) + I_{m+n+1}(kr)],\end{aligned} \tag{8a}$$

$$\begin{aligned}\Psi_{m,n}(kr) &= [K_{m+1}(kr) - K_{m-1}(kr)][I_{m-n}(kr) - I_{m+n}(kr)] \\ &\quad + K_m(kr)[I_{m-n-1}(kr) - I_{m-n+1}(kr) - I_{m+n-1}(kr) + I_{m+n+1}(kr)].\end{aligned} \tag{8b}$$

Expression (7b) will be used in combination with the boundary condition for the tangential velocity component from (1c) to find the numerical values of the truncated set of coefficients B_m. We note that the wall–normal velocity boundary condition will be then satisfied by construction. We remark that formulation (7)–(8) involves double sums, but only a single set of coefficients, which may be acceptable for the problem of determining the expansion coefficients, but is rather inefficient when the velocity components need to be evaluated at a dense grid of points in the flow domain. Therefore, for such post–processing purposes the single–sum formulation (4)–(5) will be used.

Matching (7b) against the tangential component of velocity boundary condition (1c) and truncating the series at $m = N$ and $n = N + 1$ we obtain the following algebraic system [8]

$$\sum_{m=0}^{N} B_m \lambda_{m,n}(k) = \begin{cases} 4, & (n = 1), \\ 0, & \text{otherwise,} \end{cases} \tag{9}$$

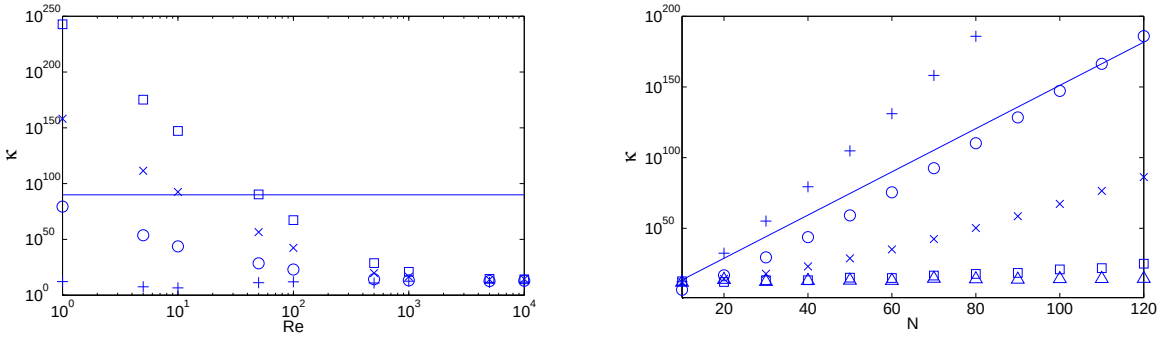

Fig. 2 Condition number κ for system (9) (a) as a function of the Reynolds number for different fixed N: (+) $N = 10$, (∘) $N = 40$, (×)$N = 70$, and (□) $N = 100$, and (b) as a function of truncation N for different fixed Reynolds numbers (+) $Re = 1$, (∘) $Re = 10$, (×) $Re = 100$, (□) $Re = 1,000$ and (△) $Re = 10,000$; for comparison, the condition number of the Hilbert matrix is indicated with a solid line; in Figure (a) it corresponds to a 50×50 Hilbert matrix.

where

$$\begin{aligned}\lambda_{m,n}(x) =& I_{m-n}(x)K_{m-1}(x) + I_{m+n}(x)K_{m+1}(x) + \\ &+ I_{m-n+1}(x)K_m(x) + I_{m+n-1}(x)K_m(x),\end{aligned} \tag{10}$$

which needs to be solved in order to determine the coefficients B_m, $m = 0, 1, \ldots, N$. While all past investigations [8,9,39] concerned very low values of N, in the present study we seek to solve system (9) for significant values of N. In addition to evaluation of the Bessel functions of very high order [up to $\mathcal{O}(10^3)$], the main difficulty is a very poor conditioning of the matrix in (9). Since the matrix entries $\lambda_{m,n}$ depend for all m and n on the Reynolds number Re, in Figures 2a and 2b we show the condition number κ of algebraic system (9) versus the order of truncation N and the Reynolds number Re. We note that, for a fixed truncation order N, the condition number actually decreases with the Reynolds number. However, the condition number increases with the resolution N, and we expect that in order to accurately resolve all features of the flow, for larger Reynolds numbers larger truncation orders N will have to be used. A priori, it is not obvious which effect (i.e., decrease of κ with Re, or its increase with N) will eventually prevail. This is one of the questions we seek to answer in Section 4.

Another important question is the asymptotic summability, as $M, N \to \infty$, of the series in (5). As shown in Appendix A, for the velocity components to be finite, the coefficients B_m, $m = 1, \ldots$ must have the behavior $|B_m| \sim \left(\frac{k}{2}\right)^m e^m m^{-m-1/2-\epsilon}$ for sufficiently large m and some arbitrarily small $\epsilon > 0$. This property is also verified computationally in Section 4.

Once the coefficients B_m, $m = 1, \ldots, M$ are computed, they can be used to determine a number of relevant quantities such as:

– the vorticity $\omega \triangleq \frac{1}{r}\left(\frac{\partial(r\, u_\theta)}{\partial r} - \frac{\partial u_r}{\partial \theta}\right)$ using the following relation

$$\omega(r,\theta) = \frac{\partial \chi(r,\theta)}{\partial r}\sin\theta + \frac{1}{r}\frac{\partial \chi(r,\theta)}{\partial \theta}\cos\theta, \tag{11}$$

– the drag coefficient $C_D \triangleq \frac{2F_x}{|\mathbf{u}_\infty|^2 S}$, where F_x is the drag force and S the area per unit length of the cylinder facing the flow; following [8,40], it can be conveniently computed as

$$C_D = -\frac{1}{2}\int_0^{2\pi}\left(r\frac{\partial \chi}{\partial r}\right)_{r=1} d\theta = -\pi A_0, \tag{12}$$

where χ and A_0 are defined in equation (5),
- the half–width W_R and length L_R of the separated region which is defined as a part of the flow domain Ω characterized by closed streamlines; the half–width W_R is the largest value of the y–coordinate in this region and the length L_R is the largest value of the x–coordinate less the radius of the cylinder,
- the separation angle θ_0 defined as the angle θ for which the skin friction vanishes, i.e.,

$$\tau(\theta_0) = 0, \quad \text{where} \quad \tau(\theta) = \mu \left(\frac{\partial u_\theta}{\partial r} \right)_{r=1}. \tag{13}$$

3 Inviscid Limit of Oseen Flows

An important problem concerns characterization of the flow that solutions of Oseen system (1) tend to in the limit $Re \to \infty$. The zero–viscosity limit results in a singular perturbation problem, a property which manifests itself in a different number of boundary conditions in system (1) and system (14) to be introduced below. From the point of view of the general mathematical theory, there remains a number of open questions concerning the inviscid limit of the Navier–Stokes flows and we refer the reader to the review paper [41] for some discussion. As shown below, some partial results can be obtained for the Oseen system. Dropping the dissipative term $\frac{1}{Re}\Delta\mathbf{u}$ we obtain *inviscid* Oseen system

$$\mathbf{u}_\infty \cdot \boldsymbol{\nabla}\mathbf{u} + \boldsymbol{\nabla} p = \mathbf{0} \qquad \text{in } \Omega, \tag{14a}$$

$$\boldsymbol{\nabla} \cdot \mathbf{u} = 0 \qquad \text{in } \Omega, \tag{14b}$$

$$\mathbf{n} \cdot \mathbf{u} = 0 \qquad \text{on } \partial A, \tag{14c}$$

where, we emphasize, only the wall–normal component of the velocity boundary condition has been retained. The "vorticity" form of (14a)–(14b) is particularly simple

$$\frac{\partial \omega}{\partial x} = 0 \qquad \text{in } \Omega \tag{15}$$

which means that $\omega = \omega(y)$ is constant along horizontal lines starting and ending at the obstacle (Figure 3). We now consider the streamfunction ψ_ω induced outside the wake region $\overline{W_1 \bigcup W_2}$, cf. Figure 3, by such a vorticity distribution $\omega(y)$ defined for x extending to infinity. In view of the identity $\Delta\psi_\omega = -\omega$, we have for $(x, y) \in \Omega \backslash \overline{W_1 \bigcup W_2}$

$$\begin{aligned} \psi_\omega(x,y) =& \frac{1}{4\pi} \int_0^1 \omega(\eta) \left\{ \int_{\sqrt{1-\eta^2}}^\infty \ln\left[(x-\xi)^2 + (y-\eta)^2\right] \, d\xi \right\} d\eta \\ &+ \frac{1}{4\pi} \int_{-1}^0 \omega(\eta) \left\{ \int_{\sqrt{1-\eta^2}}^\infty \ln\left[(x-\xi)^2 + (y-\eta)^2\right] \, d\xi \right\} d\eta. \end{aligned} \tag{16}$$

Direct calculation shows that the "inner" improper integrals $\int_{\sqrt{1-\eta^2}}^\infty \ln\left[(x-\xi)^2 + (y-\eta)^2\right] \, d\xi$ are in fact unbounded. Introducing the assumption that the vorticity ω is an *odd* function of y, i.e.,

$$\begin{aligned} \omega(-y) &= -\omega(y), \qquad \text{for } 0 \le y \le 1, \\ \omega(y) &= 0 \qquad\qquad\ \ \text{for } |y| > 1, \end{aligned} \tag{17}$$

we can combine the two integrals in (16) obtaining

$$\psi_\omega(x,y) = \frac{1}{4\pi} \int_0^1 \omega(\eta) \left[\int_{\sqrt{1-\eta^2}}^\infty \ln \frac{1 + \left(\frac{y-\eta}{x-\xi}\right)^2}{1 + \left(\frac{y+\eta}{x-\xi}\right)^2} \, d\xi \right] d\eta, \tag{18}$$

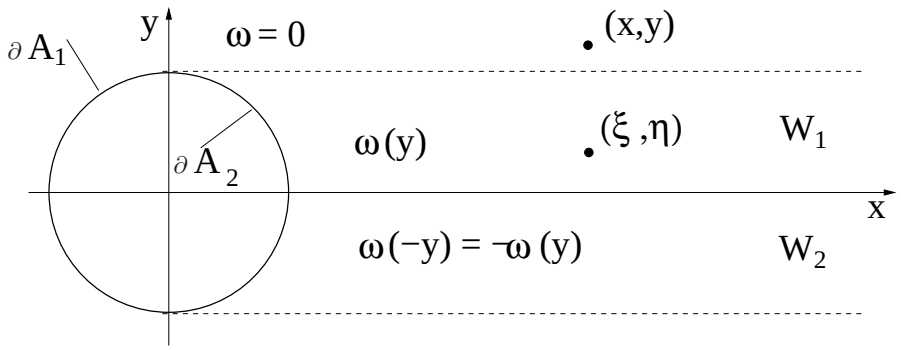

Fig. 3 Schematic vorticity distribution in the solution of inviscid Oseen problem (14)–(15).

where by direct calculation we note that the "inner" improper integral $\int_{\sqrt{1-\eta^2}}^{\infty} \ln \frac{1+\left(\frac{y-\eta}{x-\xi}\right)^2}{1+\left(\frac{y+\eta}{x-\xi}\right)^2}\, d\xi$ is now bounded (the actual expression for this integral is long and not important for the present argument, hence will be skipped). The reason is that in view of assumption (17) the unbounded contributions from the vorticity below and above the flow centerline now cancel out in (18). Thus, we conclude that all sufficiently regular distributions $\omega = \omega(y)$ with property (17) satisfy system (14), a case of lack of uniqueness characteristic of inviscid flows with vorticity, cf. e.g. [42]. Given the infinite number of inviscid Oseen flows corresponding to different distributions $\omega(y)$, the main question now is how to find the one which the solutions of *viscous* Oseen system (1) actually tend to as $Re \to \infty$. In order to answer this question, we follow the argument put forward (in 3D) by Stewartson [38] according to which the limiting solution can be found by imposing an additional boundary condition on the tangential velocity component, but only on the rear part of the obstacle boundary (∂A_2 in Figure 3), i.e.,

$$\boldsymbol{\tau} \cdot \mathbf{u} = 0 \qquad \text{on } \partial A_2, \tag{19}$$

where $\boldsymbol{\tau}$ is the unit vector tangent to the boundary. Solutions to the problem defined by (14) and (19) are computed in Section 4 and demonstrate that this problem indeed appears to be the proper inviscid limit of Oseen system (1).

4 Computational Results

As discussed in Section 2, the main difficulty in obtaining solution to the problem is poor conditioning of algebraic system (9). Because of this issue, one cannot solve problem (9) even for modest values of $N = \mathcal{O}(10^2)$ using ordinary tools of numerical linear algebra in the standard (double) precision. We attempted to address this issue using a number of alternative approaches [43], namely,

- reformulation of system (9) as a least–squares minimization problem with Tikhonov regularization,
- enforcement of boundary condition (7b) with the collocation method on different nonuniform grids instead of the Galerkin approach leading to (9),
- performing the LU decomposition in closed form based on series expansions for the entries $\lambda_{m,n}\left(\frac{Re}{4}\right)$, and
- reformulating the expansions in a way not involving the products of Bessel functions,

however, none of these approaches lead to satisfactory results in terms of accuracy. Therefore, we decided to deal with the problem of poor conditioning using sufficiently increased arithmetic precision. Thus, for every value of the Reynolds number Re we need to determine the following two numerical parameters

- the truncation order $\tilde{N}$ ensuring that truncated expansions (4)–(5), or (7)–(8), accurately represent the solution of problem (1),

– the arithmetic precision, represented by the number of significant digits $\tilde{P}$, required to obtain an accurate solution of system (9) for the given $\tilde{N}$ and Re.

For every value of Re, the quantities $\tilde{N}$ and $\tilde{P}$ are determined based on the following set of *a posteriori* checks applied to solution (7) obtained from (9) for different values of N and P

1. first, we examine the quantities

$$\begin{aligned} \Delta u_r^N &\triangleq \|u_r^{N+1} - u_r^N\|_{L_\infty(\Omega)}, \\ \Delta u_\theta^N &\triangleq \|u_\theta^{N+1} - u_\theta^N\|_{L_\infty(\Omega)}, \end{aligned} \qquad \text{as functions of } N, \tag{20}$$

   where u_r^N and u_θ^N denote expressions (7a) and (7b) truncated to N terms; the norm $L_\infty(\Omega)$ is computed discretizing the unbounded domain Ω using a finite number of grid points; expressions (20) therefore measure the magnitudes of the N–th terms in the sums in formulas (7); a solution is declared "resolved" when Δu_r^N and Δu_θ^N drop below certain prescribed tolerance, which in turn allows us to determine the minimum number $\tilde{N}$ of terms required,
2. for the truncation order $\tilde{N}$ determined in test 1. we examine

$$\|u_r^{\tilde{N}}\|_{L_\infty(\Gamma)}, \|u_\theta^{\tilde{N}}\|_{L_\infty(\Gamma)}, \qquad \text{as functions of } P \tag{21}$$

   which allows us to assess the effect of the algebraic precision P on the solution of the truncated problem; expressions (21) measure how accurately boundary conditions (1c) are satisfied; we note that the norm $\|\cdot\|_{L_\infty(\Gamma)}$ is approximated using discrete points on the boundary Γ whose number is much larger than N; this test thus allows us to determine the arithmetic precision $\tilde{P}$ needed to solve the problem with the required accuracy for the given truncation order $\tilde{N}$,
3. for the truncation order $\tilde{N}$ and arithmetic precision $\tilde{P}$ determined in tests 1. and 2. we examine

$$|B_m|, \qquad \text{as function of } m \tag{22}$$

   to establish whether the rate of decay of the coefficients B_m is fast enough to guarantee the absolute convergence of series (7), see Appendix A for the derivation of the relevant criteria.

In order to double–check consistency of the results, our computations were performed with the variable precision arithmetic both in Maple 13 and in `python` (using the `mpmath` library [44]). Inviscid problem defined by (14) and (19) is solved with a 2D version of the approach proposed originally by Stewartson [38] with the drag coefficient computed as described in [40].

Results of diagnostic tests 1.–3. are shown in Figures 4, 5 and 6. As regards the data shown in Figure 4, we add that a truncation order N is deemed acceptable, and denoted $\tilde{N}$, if the quantities Δu_r^N and Δu_θ^N drop to the level of $\mathcal{O}(10^{-16})$ [since the flow velocities are $\mathcal{O}(1)$, this means that $\Delta u_r^{\tilde{N}}$ and $\Delta u_\theta^{\tilde{N}}$ become insignificant in the double precision]. As regards the data shown in Figure 5, we look for the arithmetic precision P which ensures that the error in satisfying the boundary conditions is at most $\mathcal{O}(10^{-16})$ [which again corresponds to "zero" in the double precision when the flow quantities are $\mathcal{O}(1)$]. As regards the data shown in Figure 6, we observe rapid decay of the coefficients B_m, $m = 1, \ldots, \tilde{N}$, for all Reynolds numbers tested. In each case the decay is in fact faster than the slowest decay rate guaranteeing absolute convergence of the series, cf. relation (25), which is also indicated in Figures 6(a-g). This observation provides support for the convergence of series (5) for all Reynolds numbers tested. We also note that the range of magnitudes spanned by these coefficients increases rapidly with the Reynolds number and becomes quite large. Accurate evaluation of expansions with coefficients of such widely varying magnitudes is what necessitates the use of unusually high arithmetic precisions $\tilde{P}$.

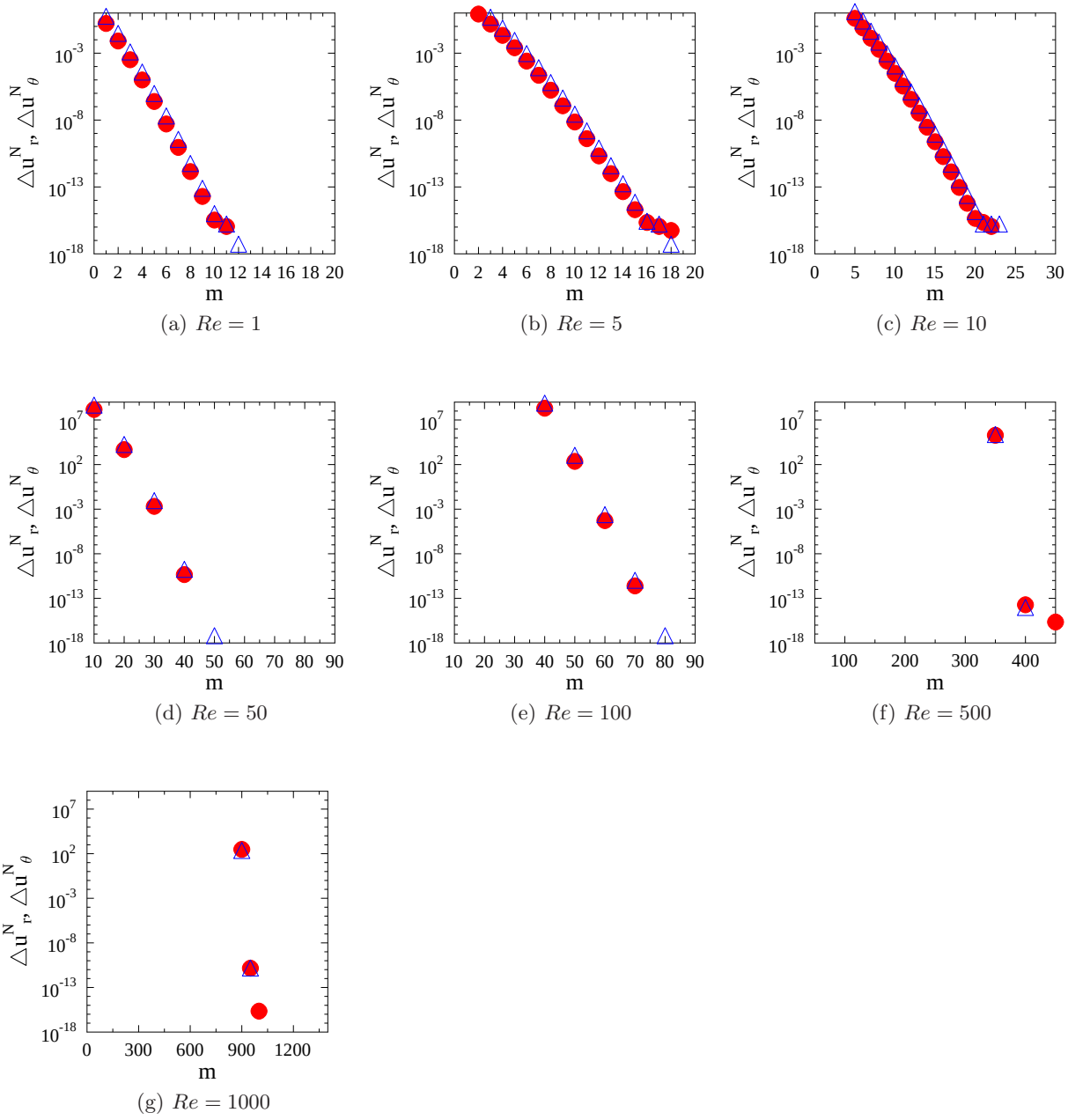

(a) $Re = 1$ (b) $Re = 5$ (c) $Re = 10$

(d) $Re = 50$ (e) $Re = 100$ (f) $Re = 500$

(g) $Re = 1000$

Fig. 4 A posteriori test 1.: quantities (•) Δu_r^N and (△) Δu_θ^N shown as functions of the truncation order N for the Reynolds numbers indicated; due to significant computational cost required to accurately evaluate the norm $\|\cdot\|_{L_\infty(\Omega)}$, for higher values of the Reynolds number the quantities Δu_r^N and Δu_θ^N are computed for some values of N only, hence in Figures (d)–(g) fewer data points are visible.

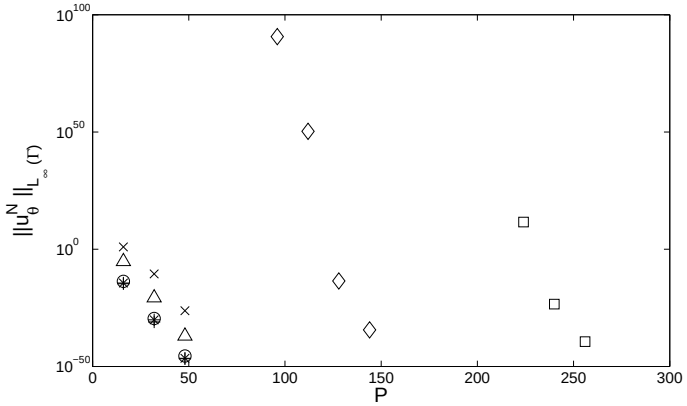

Fig. 5 A posteriori test 2.: error residual $\|u_\theta^{\tilde{N}}\|_{L_\infty(\Gamma)}$ in the satisfaction of boundary condition (7b) as a function of arithmetic precision P for different Reynolds numbers (+) $Re = 1$, (∗) $Re = 5$, (∘) $Re = 10$, (△) $Re = 50$, (×) $Re = 100$, (⋄) $Re = 500$ and (□) $Re = 1000$; the corresponding truncation orders $\tilde{N}$ are indicated in Table 1; we remark that condition $\|u_r^{\tilde{N}}\|_{L_\infty(\Gamma)} = 0$ is satisfied down to the arithmetic precision P used.

Re	N	P
1	13	32
5	19	32
10	24	32
50	60	32
100	90	48
500	500	144
1000	1000	240

Table 1 Optimal truncation orders $\tilde{N}$ and optimal arithmetic precisions $\tilde{P}$ determined for different Reynolds numbers in tests 1. and 2.

The optimal truncation orders $\tilde{N}$ and arithmetic precisions $\tilde{P}$ determined to achieve the accuracy levels mentioned above for all values of Re are collected in Table 1. In the solution of the inviscid problem defined in (14) and (19) we used 2000 complex Laurent polynomials.

We now proceed to discuss the flow patterns obtained for the different Reynolds numbers. In Figure 7 we show the velocity and vorticity fields together with streamlines (the latter in the separated regions only) in the near wake corresponding to increasing values of the Reynolds number Re and including the limiting inviscid flow discussed in Section 3. Data from Figure 7 is synthesized in Figure 8 which shows a comparison of the shapes of the separation zones for different Reynolds numbers. In all these Figures we observe progressive elongation of the separated region accompanied by thinning of the separating shear layers as the Reynolds number increases. An interesting feature of the inviscid flow evident in Figures 7o, 7p and 8 is that the separated region is in fact slightly wider than the region with nonzero vorticity, cf. (17). The half–width of the separated region in the inviscid flow was determined numerically to be about 1.07.

Moving on to discuss quantitative data, in Figures 9a,b we show the dependence of the length L_R and half–width W_R of the separation zone on the Reynolds number Re. To relate these results to the questions about the asymptotic wake structure mentioned in Introduction, in Figures 9a,b we also present the data corresponding to the Navier–Stokes solutions obtained by Fornberg [25], and by Fornberg [26] and Gajjar & Azzam [27] in the case of flows past a row of cylinders in the limit of a large distance between individual obstacles. We note in Figures 9a and 9b that while the recirculation length L_R in the viscous Oseen flows grows with the Reynolds number approximately linearly, the half–width

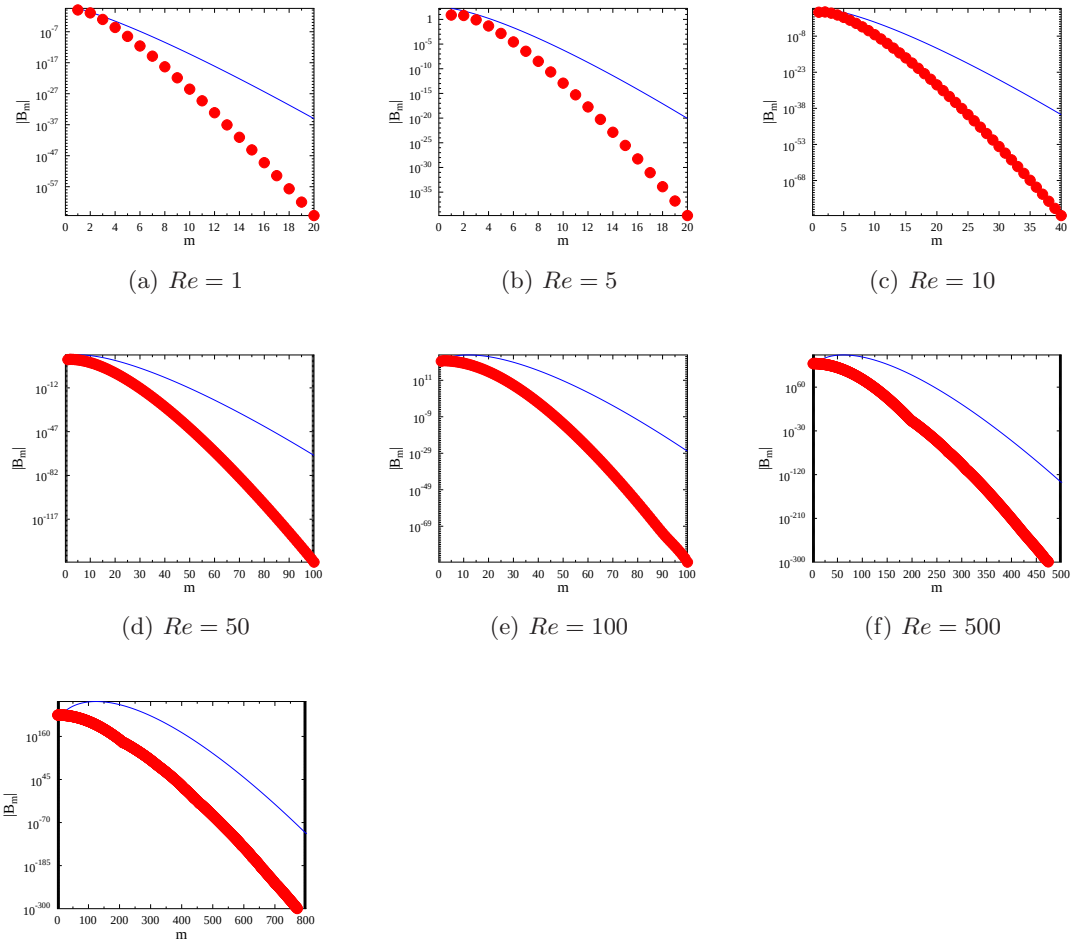

(a) $Re = 1$ (b) $Re = 5$ (c) $Re = 10$

(d) $Re = 50$ (e) $Re = 100$ (f) $Re = 500$

(g) $Re = 1000$

Fig. 6 A posteriori test 3.: magnitude of expansion coefficients $|B_m|$ as a function of m for different Reynolds numbers indicated; the solid lines represent estimate (25) with $\epsilon = 0.0$ and the constant C chosen arbitrarily in each case; the values of $\tilde{N}$ and $\tilde{P}$ are indicated in Table 1.

W_R of the separated region rapidly approaches the limiting value of 1.07 which characterizes the inviscid Oseen flow. In the Navier–Stokes flows computed by Fornberg [25,26] and Gajjar & Azzam [27] the recirculation length exhibits similar trends to the Oseen flows, but on the other hand, the half–width W_R grows much more rapidly. In Figure 9c, showing the dependence of the drag coefficient C_D on the Reynolds number, we note that in the limit $Re \to \infty$ the drag in the viscous Oseen flows approaches a finite value corresponding to the inviscid flow. Evidently, solutions of the inviscid Oseen problem are not subject to "D'Alembert's paradox", as is also the case for the Kirchhoff free–streamline solutions of the Euler equations [17,18]. At small values of the Reynolds number we compare the values of the drag coefficient C_D, cf. (12), with the approximate expressions due to Bairstow et al. [46] and Lamb [3] which are based on low–order truncations of the solutions to the Oseen system. We also observe that the drag coefficient in the Navier–Stokes flows computed by Fornberg [25,26] is significantly lower and exhibits a rather different trend, namely, it appears to vanish as $Re \to \infty$ (see also the discussion in [31]). On the other hand, in the Navier–Stokes solutions computed by Gajjar & Azzam [27] and corresponding to flows past a row of cylinders the drag coefficient C_D appears to approach a finite

value as $Re \to \infty$. It should be, however, noted that as regards the behavior of the drag coefficient the flow past a row of obstacles represents a fundamentally different problem. The results can be directly compared to those for the flow past a single body only in the limit of a large distance between the obstacles, a case which was not studied in [27] due to numerical difficulties. Finally, in Figure 9d we show the separation angle θ_0, cf. (13), as a function of Re. For comparison, we also indicate the value of the separation angle characterizing the inviscid Oseen flow, $\theta_0 = 90$deg, and the results obtained by Fornberg for the Navier–Stokes system [24] (we were not able to obtain this data for other numerical studies referenced here). We note that, in contrast to the diagnostics examined above, the separation angle θ_0 in the viscous Oseen flows exhibits rather slow convergence to the angle obtained in the inviscid flow.

5 Conclusions and Discussions

Motivated by the results of the mathematical analysis demonstrating the connection between steady Navier–Stokes flows past obstacles in unbounded domains and Oseen flows, we offer a careful characterization of the solutions of the 2D Oseen system for a broad range of the Reynolds number and including also the limiting inviscid case. The solutions to the 2D Oseen problem were computed based on the series expansions due to Tomotika and Aoi [8]. The severe ill–conditioning of the associated algebraic problem and the need to evaluate accurately high–order Bessel functions were overcome by performing all algebraic operations with a sufficiently high arithmetic precision. For every Reynolds number this precision was chosen independently together with the truncation level for the series in order to meet quite stringent criteria for the accuracy of the solution. Our results provide computational evidence, at least for the range of the Reynolds numbers investigated (i.e., from 1 to 1,000), for the actual convergence of Tomotika and Aoi's infinite series whose derivation was only formal [8]. We also show that the solution of the inviscid Oseen problem proposed by Stewartson [38] indeed appears to be the appropriate limit of the viscous Oseen flows as $Re \to \infty$. This is confirmed by the convergence of a number of diagnostics, namely, the half–width W_R of the separated region, drag coefficient C_D and the separation angle θ_0, to the values characterizing the inviscid solution (although in the case of the separation angle this convergence is rather slow). This appears to be an interesting result as there are not many nontrivial problems in fluid dynamics where the inviscid limit in known. We add that the inviscid Oseen flows share a number of important features with Kirchhoff free–streamline flows [17,18] such as unbounded separated region and nonzero drag.

The results obtained, together with the mathematical facts discussed in Introduction, may allow for some observations to be made about the steady Navier–Stokes flows computed by Fornberg [25]. It appears that, at least as regards the structure of the separated region, for Reynolds numbers up to about 300 those flows exhibit a number of similarities with the Oseen flows. This is however no longer the case for Reynolds numbers above 300, where those flows feature a wide separated region, quite unlike the slender Oseen wakes.

Acknowledgments

The authors acknowledge the funding for this research provided by NSERC (Discovery Grant) and SHARCNET (graduate scholarship). The authors are grateful to Prof. S. Chernyshenko for interesting discussions concerning the asymptotic theory of global separation. They also wish to thank Dr. Ramesh Yapalparvi for discussions and comments on an earlier draft of this work.

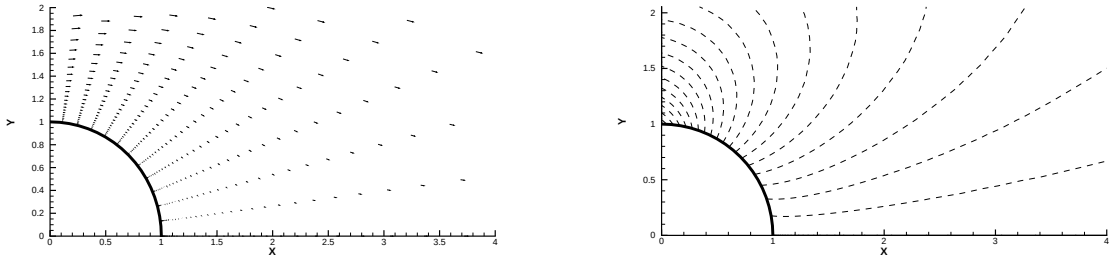

(a) $Re = 1$ (b) $Re = 1$

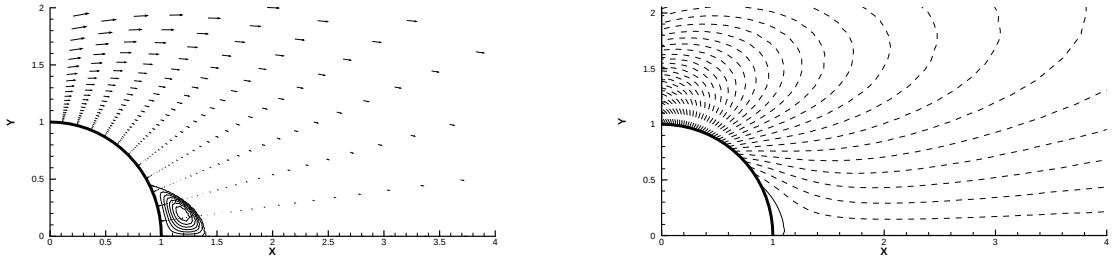

(c) $Re = 5$ (d) $Re = 5$

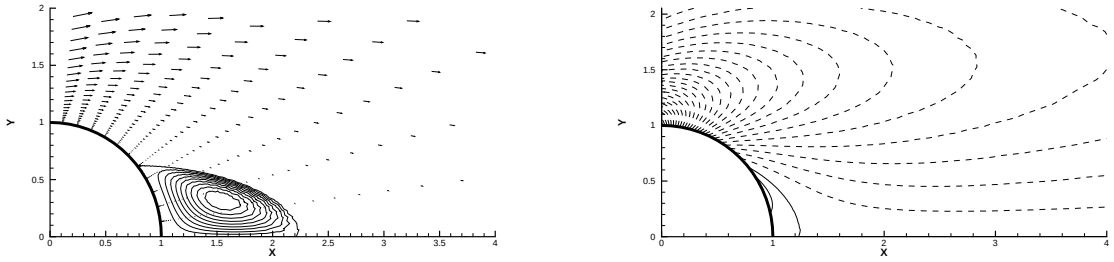

(e) $Re = 10$ (f) $Re = 10$

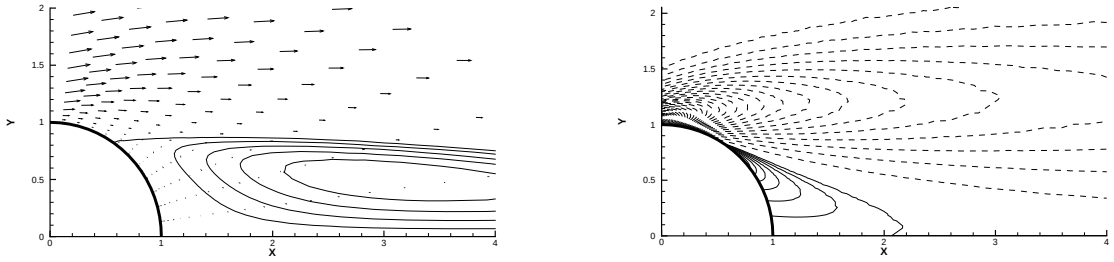

(g) $Re = 50$ (h) $Re = 50$

Fig. 7 (Left column) velocity fields and streamline patterns and (right column) vorticity fields in Oseen flows for the Reynolds numbers indicated; for clarity, the streamlines are shown only in the separated regions; in the vorticity plots isocontours corresponding to positive and negative vorticity are indicated with solid and dashed lines, respectively.

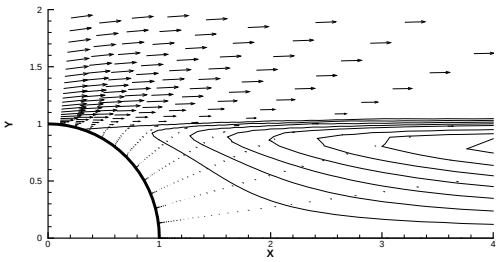

(i) $Re = 100$

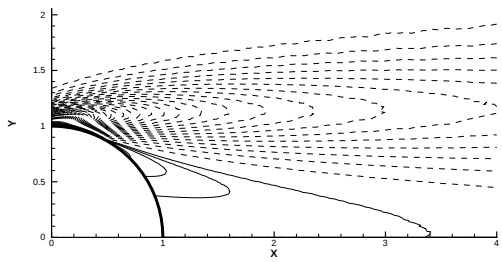

(j) $Re = 100$

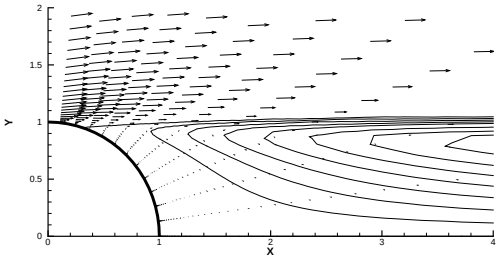

(k) $Re = 500$

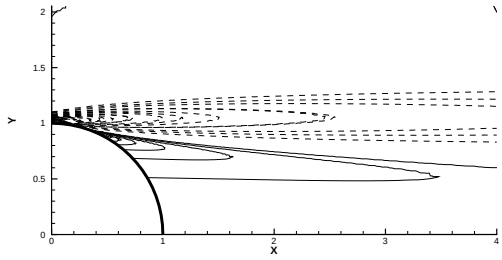

(l) $Re = 500$

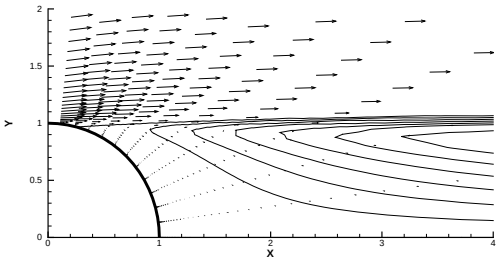

(m) $Re = 1000$

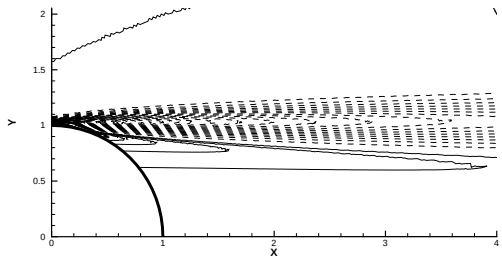

(n) $Re = 1000$

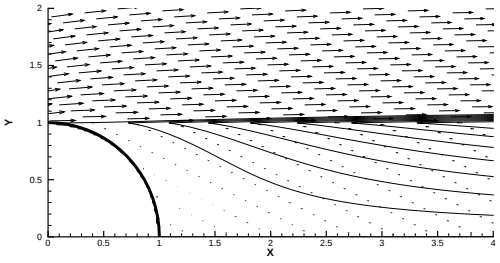

(o) $Re = \infty$

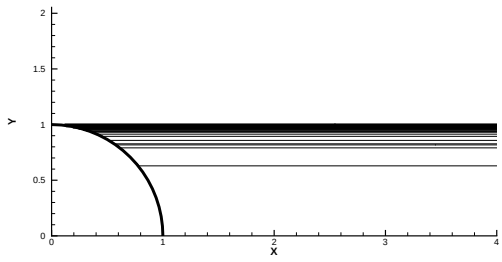

(p) $Re = \infty$

Fig. 7 (Continued, see previous caption for details); Figures (o) and (p) represent solutions of inviscid problem defined by (14) and (19).

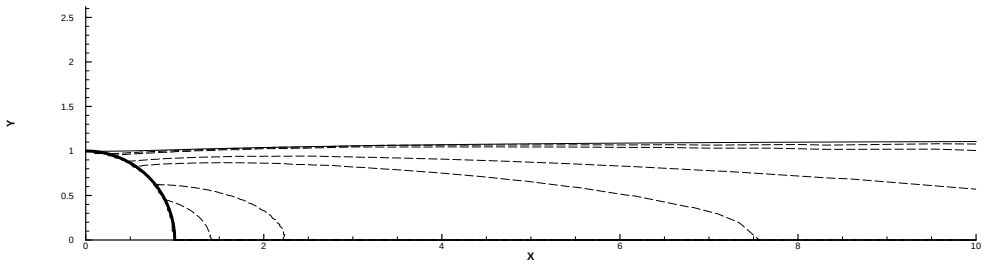

Fig. 8 (Dashed lines) boundaries of the the separated regions in Oseen flows with the Reynolds numbers $Re = 5, 10, 50, 100, 500, 1000$ (longer bubbles correspond to higher Reynolds numbers); solid line represents the boundary of the separated region in inviscid problem (14)–(19).

A Criteria for Convergence of Series in (5)

Here we establish the slowest asymptotic decay rates of the coefficients A_n and B_m, $m, n = 1, \ldots$ that will guarantee the boundedness of the velocity field given by representation (4). We note that this requires the absolute summability of the *derivatives* (with respect to r and θ) of the series in (5). As regards the summation in (5b), we thus have for any fixed $r \geq 1$ and $\epsilon > 0$

$$\left| n \frac{A_n \cos(n\theta)}{n r^n} \right| \leq \frac{|A_n|}{r^n} \leq |A_n| \quad \Longrightarrow \quad |A_n| \sim n^{-1-\epsilon} \text{ as } n \to \infty. \tag{23}$$

As regards the summation in (5a), we use the following asymptotic property of the modified Bessel function of the second kind [45],

$$K_m(kr) \sim \sqrt{\frac{\pi}{2m}} e^{-m} \left(\frac{kr}{2m} \right)^{-m} \quad \text{as } m \to \infty \tag{24}$$

which holds for fixed $k > 0$ and $r \geq 1$, so that we obtain

$$\begin{aligned} &\left| m\, B_m\, K_m(kr)\, \cos(m\theta) \right| \leq m\, |B_m|\, K_m(kr) \leq C\, |B_m| \left(\frac{k}{2} \right)^{-m} \frac{e^{-m}}{m^{-m-1/2}} \\ &\Longrightarrow \quad |B_m| \sim \left(\frac{k}{2} \right)^{m} e^m m^{-m-1/2-\epsilon} \text{ as } m \to \infty, \end{aligned} \tag{25}$$

where $C > 0$ is a constant. We note that conditions (23) and (25) have to be satisfied for the velocity components to be finite, and for velocity derivatives to be finite, the absolute values of the coefficients B_m have to go towards zero faster. Finally, we add that neither estimate (23) nor (25) is sharp.

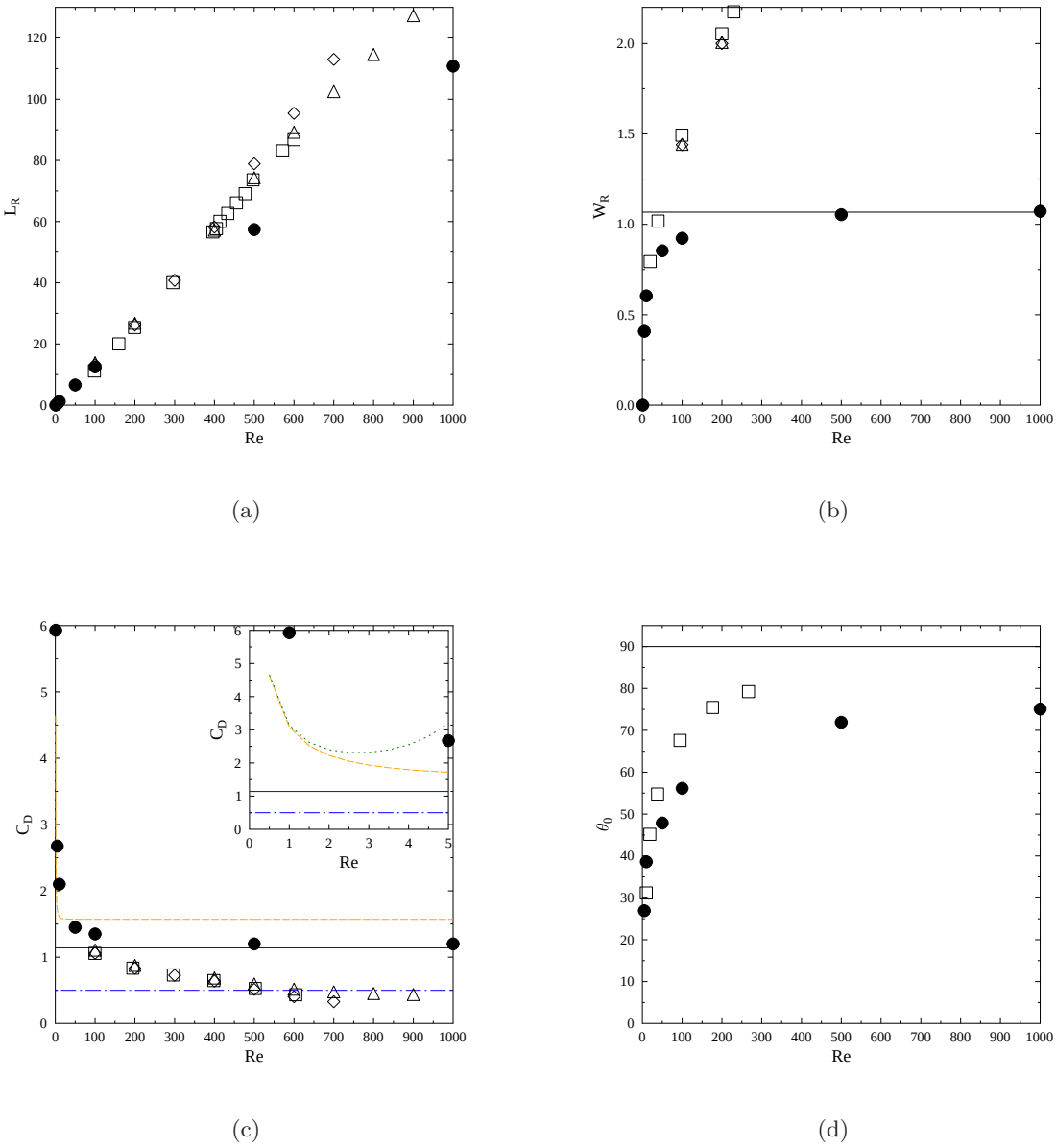

Fig. 9 (a) Length L_R and (b) half–width W_R of the separated region, (c) drag coefficient C_D and (d) the separation angle θ_0 as functions of the Reynolds number Re; in all Figures circles represent the present results for the viscous Oseen problem, whereas the solid line corresponds to the inviscid Oseen flow, squares and diamonds correspond to the results of Fornberg, respectively from [25] and [26], triangles correspond to the results of Gajjar & Azzam [27] for the case where the distance between the obstacles is 100 cylinder radii; in Figure (c) dashed and dotted lines represent the approximate formulas due to Bairstow et al. [46] and Lamb [3], whereas the dash–dotted line corresponds to the drag coefficient in the Kirchhoff free–streamline flow [31, 17, 18].

References

1. S. Childress, *An Introduction to Theoretical Fluid Mechanics*, American Mathematical Society, (2009).
2. R. B. Guenther and E. A. Thomann, "Fundamental Solutions of Stokes and Oseen Problem in Two Spatial Dimensions", *Journal of Mathematical Fluid Mechanics* **9**, 489-505, (2006).
3. H. Lamb, "On the uniform motion of a sphere through a viscous fluid ", *Philos. Mag.* **21**, 112, (1911).
4. C. W. Oseen, "Über die Stokes'sche formel, und über eine verwandte Aufgabe in der Hydrodynamik", *Ark. Mat., Astron. Fys.* **9**, 1, (1913)
5. R. W. Burgess, "The Uniform Motion of a Sphere through a Viscous Liquid", *Am. J. Math.* **38**, 81, (1916).
6. H. Faxén, "Exakte Lösung der Oseen schen Differentialgleichungen einer zhen Flüssigkeit für den Fall der Translationsbewegung eines Zylinders", *Nova Acta Regiae Soc. Sci. Ups.*, Volumen extra ordine, **1**, 1–55, (1927).
7. S. Goldstein, ''The steady flow of viscous fluid past a fixed spherical obstacle at small Reynolds numbers", *Proc. R. Soc. London, Ser. A* **123**, 225, (1929).
8. S. Tomotika and T. Aoi, "The Steady Flow of Viscouis Fluid Past a Sphere and Circular Cylinder at Small Reynolds Numbers", *Q. J. Mech. Appl. Math.* **3**, 140–161, (1950).
9. S. C. R. Dennis and S. Kocabiyik, "The Solution of Two–Dimensional Oseen Flow problems Using Integral Conditions", *IMA Journal of Applied Mathematics* **45**, 1–31, (1990).
10. E. Chadwick, "The Far–Field Oseen Velocity Expansion", *Proc. R. Soc. London, Ser. A* **454**, 2059–2082, (1998).
11. N. Fishwick and E. Chadwick, "The evaluation of the far–field interal in the Green's function representation for steady Oseen flow", *Physics of Fluids* **18**, 113101, (2006).
12. E. R. Lindgren, "The motion of a sphere in an incompressible viscous fluid at Reynolds numbers considerably less than one", *Phys. Scr.* **60**, 97, (1999)
13. J. Veysey II and N. Goldenfeld, "Simple viscous flows: From boundary layers to the renormalization group", *Reviews of Modern Physics* **79**, 883–927, (2007).
14. S. A. Berger, *Laminar Wakes*, Elsevier, (1971).
15. F. Abraham, M. Behr and M. Heinkenschloss, "The Effect of Stabilization in Finite Element Methods for the Optimal Boundary Control of the Oseen Equations", *Finite Elements in Analysis and Design*, **41**, 229–251, (2004).
16. C.-X. Zheng and H.-D. Han, "The artificial boundary conditions for exterior oseen equation in 2-D space", *Journal of Computational Mathematics* **20**, 591–598, (2002).
17. T. Levi–Civita, "Scie e leggi di reistenza", *Rendiconti del Circolo Matematico di Palermo* **XXIII**, 1–37, (1907).
18. S. Brodetsky, "Discontinuous fluid motion past circular and elliptic cylinders", *Proc. R. Soc. London, Ser. A* **102**, 542, (1923).
19. G. Batchelor, "A proposal concerning laminar wake behind bluff bodies at large Reynolds numbers", *J. Fluid Mech.* **1**, 388–398, (1957).
20. S. I. Chernyshenko, "The asymptotic form of the stationary separated circumfluence of a body at high Reynolds number", *Prikl. Matem. Mekh.* **52**, 958–966, (1988).
21. S. I. Chernyshenko, "Asymptotic theory of global separation", *Appl. Mech. Rev.* **51**, 523–536, (1998).
22. S. I. Chernyshenko and I. P. Castro, "High–Reynolds–number asymptotics of the steady flow through a row of bluff bodies", *J. Fluid Mech.* **257**, 421–449, (1993).
23. S. I. Chernyshenko and I. P. Castro, "High–Reynolds number weakly stratified flow past an obstacle", *J. Fluid Mech.* **317**, 155–178, (1996).
24. B. Fornberg, "A numerical study of steady viscous flow past a circular cylinder", *J. Fluid Mech.* **98**, 819–855, (1980).
25. B. Fornberg, "Steady viscous flow past a circular cylinder up to Reynolds number 600", *Journal of Computational Physics* **61**, 297–320, (1985).
26. B. Fornberg, "Steady incompressible flow past a row of circular cylinders", *J. Fluid Mech.* **225**, 655–671, (1991).
27. J. S. B. Gajjar and N. A. Azzam, "Numerical solution of the Navier–Stokes equations for the flow in a cylinder cascade", *J. Fluid Mech.* **520**, 51–82, (2004).
28. S. Sen, S. Mittal and G. Biswas, "Steady separated flow past a circular cylinder at low Reynolds numbers", *J. Fluid Mech.* **620**, 89–119, (2009).
29. B. Fornberg, "Steady viscous flow past a sphere at high Reynolds numbers", *J. Fluid Mech.* **190**, 471–489, (1988).
30. B. Fornberg, "Computing steady incompressible flows past blunt bodies — A historical overview", in *Numerical Methods for Fluid Dynamics IV* (Ed. M.J. Baines and K.W. Morton) Oxford Univ. Press, 115–134, (1993).

31. V. V. Sychev, A. I. Ruban, V. V. Sychev and G. L. Korolev, *Asymptotic Theory of Separated Flows*, Cambridge University Press, (1998).
32. R. Finn, "On the Exterior Stationary Problem for the Navier–Stokes Equations, and Associated Perturbation Problems", *Arch. Rational Mech. Anal.* **19**, 363–406, (1965).
33. D. Smith, "Estimates at Infinity for Stationary Solutions of the Navier–Stokes Equations in Two Dimensions", *Arch. Rational Mech. Anal.* **20**, 341–372, (1965).
34. G. Galdi, *An Introduction to the Mathematical Theory of Navier–Stokes Equations, Vol. I: Linearized Steady Problems, Vol. II: Nonlinear Steady Problems*, Springer, (1994).
35. R. Mizumachi, "On the asymptotic behavior of incompressible viscous fluid motion past bodies", *J. Math. Soc. Japan* **36**, 497–522, (1984).
36. S. Bönisch, V. Heuveline and P. Wittwer, "Adaptive boundary conditions for exterior flow problems", *Journal of Mathematical Fluid Mechanics* **7**, 85–107, (2005).
37. S. Bönisch, V. Heuveline and P. Wittwer, "Second order adaptive boundary conditions for exterior flow problems: non–symmetric stationary flows in two dimensions", *Journal of Mathematical Fluid Mechanics* **9**, 1–26, (2007).
38. K. Stewartson, "On the Steady Flow past a Sphere at High Reynolds Number using Oseen's Approximation", *Phil. Mag* **1**, 345–354, (1956).
39. S. M. Abane, "Calculation of Oseen Flows Past a Circular Cylinder it Low Reynolds Numbers", *Appl. Sci. Res.* **34**, 413–426, (1978).
40. A. J. Weisenborn and B. I. M. Ten Bosch, "The Oseen Drag at Infinite Reynolds number", *SIAM Journal on Applied Mathematics* **55**, 1227–1232, (1995).
41. W. E, "Boundary Layer Theory and the Zero–Viscosity Limit of the Navier–Stokes Equation", *Acta Mathematica Sinica, English Series* **16**, 207–218, (2000).
42. A. Elcrat, B. Fornberg, M. Horn & K. Miller, "Some steady vortex flows past a circular cylinder", *J. Fluid Mech.* **409**, 13-27, (2000).
43. P. Ch. Hansen, *Rank–Deficient and Discrete Ill–Posed Problems. Numerical Aspects of Linear Inversion*, SIAM, (1998).
44. F. Johansson et al., *mpmath: a Python library for arbitrary-precision floating-point arithmetic (version 0.17)*, `http://code.google.com/p/mpmath/`, (2011).
45. F. W. J. Oliver, D. W. Lozier, R. F. Boisvert and C. W. Clarke, *NIST Handbook of Mathematical Functions*, Cambridge University Press, (2010).
46. L. Bairstow, B. M. Cave, and E. D. Lang, "The Resistance of a Cylinder Moving in a Viscous Fluid", *Philosophical Transactions of the Royal Society of London. Series A, Containing Papers of a Mathematical or Physical Character* **223**, 383–432, (1923)